

Rebound Potentiation of Inhibition in Juvenile Visual Cortex Requires Vision-Induced BDNF Expression

Ming Gao,^{1,2} Kristen R. Maynard,³ Varun Chokshi,¹ Lihua Song,^{1,2} Cara Jacobs,² Hui Wang,¹ Trinh Tran,¹
 Keri Martinowich,^{3,4} and Hey-Kyoung Lee^{1,2}

¹The Solomon H. Snyder Department of Neuroscience, The Zanvyl-Krieger Mind/Brain Institute, Johns Hopkins University, Baltimore, Maryland 21218, ²Department of Biology, University of Maryland, College Park, Maryland 20742, ³Lieber Institute for Brain Development, Baltimore, Maryland 21205, and ⁴Department of Psychiatry and Behavioral Sciences, Johns Hopkins University School of Medicine, Baltimore, Maryland 21205

The developmental increase in the strength of inhibitory synaptic circuits defines the time window of the critical period for plasticity in sensory cortices. Conceptually, plasticity of inhibitory synapses is an attractive mechanism to allow for homeostatic adaptation to the sensory environment. However, a brief duration of visual deprivation that causes maximal change in excitatory synapses produces minimal change in inhibitory synaptic transmission. Here we examined developmental and experience-dependent changes in inhibition by measuring miniature IPSCs (mIPSCs) in layer 2/3 pyramidal neurons of mouse visual cortex. During development from postnatal day 21 (P21) to P35, GABA_A receptor function changed from fewer higher-conductance channels to more numerous lower-conductance channels without altering the average mIPSC amplitude. Although a week of visual deprivation did not alter the average mIPSC amplitude, a subsequent 2 h exposure to light produced a rapid rebound potentiation. This form of plasticity is restricted to a critical period before the developmental change in GABAergic synaptic properties is completed, and hence is absent by P35. Visual experience-dependent rebound potentiation of mIPSCs is accompanied by an increase in the open channel number and requires activity-dependent transcription of brain-derived neurotrophic factor (BDNF). Mice lacking BDNF transcription through promoter IV did not show developmental changes in inhibition and lacked rebound potentiation. Our results suggest that sensory experience may have distinct functional consequences in normal versus deprived sensory cortices, and that experience-dependent BDNF expression controls the plasticity of inhibitory synaptic transmission particularly when recovering vision during the critical period.

Key words: activity-dependent; BDNF; critical period; mIPSC; potentiation; visual cortex

Introduction

The nervous system is endowed with multiple plasticity mechanisms that allow circuits to encode sensory information and to adapt to alterations in the sensory environment. Synaptic mechanisms of sensory plasticity have been most prominently studied in the primary visual cortex (V1), where a brief period of visual deprivation during an early critical period leads to permanent changes in cortical function (Levelt and Hübener, 2012). Proper maturation of inhibitory synaptic transmission is critical for the normal development of sensory features in V1 (Li et al., 2012), and is responsible for the initiation and closure of the critical period for plasticity (Jiang et al., 2005; Levelt and Hübener, 2012). Maturation of inhibition is dependent on sensory experi-

ence, especially in the superficial layers of V1. For instance, visual deprivation from birth prevents the developmental increase in both inhibitory synaptic strength (Morales et al., 2002) and the number of inhibitory synaptic contacts (Huang et al., 1999; Chattopadhyaya et al., 2004; Kreczko et al., 2009). Visual experience plays a permissive role in initiating the developmental maturation of inhibition as only a very brief period of normal vision early on is sufficient to trigger its maturation (Morales et al., 2002). This suggests that visual experience may not be necessary for controlling inhibitory synapses once the developmental process is initiated. However, results from *in vitro* studies suggest that inhibitory synapses are malleable to regulation by changes in ongoing neuronal activity (Hartman et al., 2006; Swanwick et al., 2006; Kim and Alger, 2010), which is considered critical for maintaining homeostasis in neural networks.

Brain-derived neurotrophic factor (BDNF) expression increases gradually in the cortex over the course of development (Maisonpierre et al., 1990), and overexpression of BDNF leads to precocious maturation of inhibition and early closure of the critical period for ocular dominance plasticity (Huang et al., 1999). The *Bdnf* gene contains at least nine promoters (Aid et al., 2007), each driving transcription of an individual 5' untranslated exon spliced to a common 3' coding exon. Some of these promoters, notably promoters I and IV, are highly responsive to changes in

Received Dec. 30, 2013; revised June 30, 2014; accepted July 3, 2014.

Author contributions: K.M. and H.-K.L. designed research; M.G., K.R.M., V.C., L.S., C.J., H.W., T.T., and H.-K.L. performed research; K.M. contributed unpublished reagents/analytic tools; M.G., K.R.M., V.C., L.S., C.J., and H.-K.L. analyzed data; M.G., K.R.M., K.M., and H.-K.L. wrote the paper.

This work was supported by National Institutes of Health Grant R01-EY14882 to H.-K.L. and a grant from the Lieber Institute for Brain Development to K.M. We thank Dr. Alfredo Kirkwood for helpful discussions, and Dr. Jessica Whitt for help on the manuscript.

Correspondence should be addressed to Hey-Kyoung Lee, Johns Hopkins University, Dunning Hall Room 348, 3400 North Charles Street, Baltimore, MD 21218. E-mail: heykyounglee@jhu.edu.

M. Gao's present address: Division of Neurology, Barrow Neurological Institute, Phoenix, AZ 85013.
 DOI:10.1523/JNEUROSCI.5454-13.2014

Copyright © 2014 the authors 0270-6474/14/3410770-10\$15.00/0

neuronal activity. Exon IV-containing *Bdnf* transcripts are the most abundantly expressed *Bdnf* transcripts in the cortex, where they substantially contribute to activity-dependent production of BDNF. Disruption of BDNF production from promoter IV interferes with the sculpting of inhibition in various cortical areas (Hong et al., 2008; Sakata et al., 2009; Jiao et al., 2011). However, whether the developmental effect of BDNF on the maturation of inhibition is due specifically to activity-dependent transcription of BDNF, and the mechanism by which it regulates inhibitory synaptic transmission with sensory experience remains unknown.

Here, we report that visual experience following a period of visual deprivation produces a rebound potentiation of inhibitory synaptic strength, which is limited to a critical period. Using mice in which promoter IV-dependent BDNF production is completely disrupted (BDNF-KIV), we demonstrate that the rebound potentiation of inhibition critically depends on the expression of activity-dependent BDNF. Thus, our results highlight a critical role for activity-dependent *Bdnf* transcription in rapidly sculpting inhibitory synaptic circuits when vision is restored.

Materials and Methods

Manipulation of visual experience. Wild-type (WT) mice (C57BL/6J; The Jackson Laboratory) or BDNF-KIV mice and their WT littermates (C57BL/6J background; Sakata et al., 2009) were raised in a normally lighted environment [12 h light/dark cycle; control, i.e., normally reared (NR)] or were placed in dark exposure (DE) for a duration of 7 d initiated at postnatal day 21 (P21), P28, or P35. DE mice were cared for using infrared vision goggles under dim infrared light. Some of the DE mice were exposed to a lighted environment for 2 h (2hL), 1 d (1dL), 3dL, or 7dL to study the effect of re-exposure to light. Mice of both sexes were used for the studies.

Preparation of visual cortical slices. Each mouse was deeply anesthetized with isoflurane vapors and killed by decapitation. The brain was rapidly removed and immersed in ice-cold dissection buffer (in mM: 212.7 sucrose, 2.6 KCl, 1.23 NaH₂PO₄, 26 NaHCO₃, 10 dextrose, 3 MgCl₂, and 1 CaCl₂) saturated with a 95% O₂/5% CO₂ mixture. Blocks of primary visual cortices were rapidly dissected and sectioned into 300- μ m-thick coronal slices using a Vibratome 3000 plus microslicer (Ted Pella). The slices were gently transferred to a submersion holding chamber with artificial CSF [ACSF; (in mM): 124 NaCl, 5 KCl, 1.23 NaH₂PO₄, 26 NaHCO₃, 10 dextrose, 1.5 MgCl₂, 2.5 CaCl₂], saturated with 95% O₂/5% CO₂, and recovered at room temperature for ~1 h before recording.

Whole-cell recording of miniature IPSCs. The visual cortical slices were moved to a submersion-type recording chamber mounted on a stage of an upright microscope (E600 FN-1; Nikon) equipped with infrared oblique illumination. Miniature IPSCs (mIPSCs) were recorded in layer 2/3 pyramidal cells in the presence of 1 μ M TTX, 100 μ M D,L-APV and 10 μ M 2,3-dihydroxy-6-nitro-7-sulfonyl-benzo[*f*]quinoxaline (NBQX) and analyzed with the Mini Analysis Program (Synaptosoft). An intracellular recording solution that allows GABA_A receptor (GABA_AR)-mediated IPSCs to reverse at 0 mV (Morales et al., 2002) was used (in mM: 140 CsCl, 8 KCl, 10 EGTA, 10 HEPES, and 10 QX-314, pH 7.3). Cells were held at -80 mV to record mIPSCs using an Axopatch 700B amplifier (Molecular Devices), digitized at 2 kHz by a data acquisition board (National Instruments), and acquired using custom-made Igor Pro software (WaveMetrics). The threshold for detecting mIPSCs was set at three times the root mean square (RMS) noise. There was no significant difference in RMS noise between the experimental groups ($p > 0.2$). Cells showing a negative correlation between mIPSCs amplitude and rise time were excluded from analysis, as well as mIPSCs with a >5 ms rise time (measured between 10% and 90% of amplitude). A total of 350–500 consecutive events from each experiment were considered for the determination of mIPSC frequency, but highly superimposed events constituting “bursts” (more than two events, interevent interval <10 ms) were excluded from the measurement of amplitudes (300 nonburst events from each cell were used for average mIPSC amplitude calculations). The

decay time constant was calculated using the average of 150–200 well isolated events. Only the cells and recording conditions that met the following criteria were studied: V_m less than or equal to -65 mV at breakin, input $R \geq 200$ M Ω , and series $R \leq 25$ M Ω . Cells were discarded if input R or series R changed $>15\%$. Junction potentials were typically <5 mV, and were left uncompensated. TTX, bicuculline, DL-APV, and NBQX were purchased from Sigma-RBI.

Peak scaled nonstationary fluctuation analysis. Single-channel conductance and the number of channel were estimated by peak-scaled nonstationary noise analysis (De Koninck and Mody, 1994) using the Mini Analysis Program (Synaptosoft; Hartveit and Veruki, 2007). A plot of corresponding values of variance versus mean amplitude, for each point in time, was fitted with the following equation:

$$\sigma^2 = iI - I^2/N + b_1,$$

where σ^2 is the variance, I is the mean current, i is the single-channel current, N is the number of open channel at peak current, and b_1 is the background variance.

Single-channel conductance (γ) was calculated using the following formula:

$$\gamma = i/V,$$

where V is the driving force, which was calculated from:

$$V = |V_h - V_{rev}|.$$

Under our recording conditions, V_h , the holding potential, was -80 mV, and V_{rev} , the reversal potential for GABA_AR, was 0 mV. Only the cells where $R^2 > 0.4$ for curve fit were used for analysis.

Steady-state surface biotinylation and immunoblot analysis. Slice biotinylation experiments were conducted as previously described (Goel et al., 2011). In brief, visual cortex slices were transferred to ice-cold ACSF for 10 min after recovery and were subsequently transferred to ice-cold ACSF containing 2 mg/ml biotin (EZ-Link Sulfo-NHS-SS Biotin, Pierce) saturated with 95% O₂/5% CO₂ for 10 min. The slices were then washed in ice-cold Tris-buffered saline (50 mM Tris, 0.9% NaCl, pH 7.4) containing 100 mM glycine five times (1 min each) before being collected in ice-cold 0.2% SDS and 1% Triton X-100 immunoprecipitation buffer (TX-IPB; in mM: 20 mM Na₃PO₄, 150 mM NaCl, 10 mM EDTA, 10 mM EGTA, 10 mM Na₄P₂O₇, 50 mM NaF, and 1 mM Na₃VO₄, pH 7.4; with 1 μ M okadaic acid and 10 kIU/ml aprotinin). Slices were homogenized on ice by ~30 strokes using glass-Teflon tissue homogenizers (Pyrex) and centrifuged for 10 min at 13,200 $\times g$, and 4°C. Protein concentration of the supernatant was measured and normalized to 1 or 2 mg/ml. Some of the supernatants were saved as inputs by the addition of gel sample buffer and boiled for 5 min. Three hundred micrograms of each supernatant was mixed with neutravidin slurry (1:1 in 1% TX-IPB) and rotated overnight at 4°C. The neutravidin beads were isolated by brief centrifugation at 1000 $\times g$. Some of the supernatants were saved by adding gel sample buffer and boiled for 5 min. The neutravidin beads were washed three times with 1% TX-IPB and three times with 1% TX-IPB with 500 mM NaCl, and followed by two washes in 1% TX-IPB. The biotinylated surface proteins were eluted from the beads by boiling in gel sample buffer for 5 min. The input (total homogenate), supernatant (intracellular fraction), and biotinylated samples (surface fraction) were run on the same SDS-PAGE gel and processed for immunoblot analysis. All homogenates from each experimental animal were run on gels to compare the total expression level of GABA_AR subunits via immunoblot analysis. Primary antibodies used for immunoblots were anti- $\alpha 1$ (1:1000; ab32589, Abcam), anti-beta2/3 (1:200; MAB341, Millipore), and anti-gamma2 (1:200; sc-101963, Santa Cruz Biotechnology) diluted in blocking buffer (1% bovine serum albumin in PBS; PBS, pH 7.4). Secondary antibodies were conjugated to alkaline phosphatase, developed using enhanced chemifluorescence substrate (GE Healthcare), and scanned on a Typhoon 9400 imager (GE Healthcare). Band intensities were quantified using Image Quant TL software (GE Healthcare). The calculated total surface biotinylation signals were normalized to the total input signal to obtain the percentage of surface protein for each sample. For total ho-

mogenate blots, band intensities were normalized to the average intensity of NR samples on the same blot to obtain percentage of average NR mice.

Immunohistochemical labeling of GAD65-positive terminals and confocal imaging. Mice were deeply anesthetized with isoflurane and underwent transcardial perfusion with 4% paraformaldehyde solution in sodium phosphate buffer (in mM: 30 mM NaH₂PO₄, 120 mM Na₂HPO₄, pH 7.4). A total of three juvenile mice were used for each experimental group (NR, DE, and 7 dL). Brains were kept in 4% paraformaldehyde solution, pH 7.4, at 4°C at least overnight for up to 2 months before experimental use. The day before sectioning, brains were placed in 30% sucrose (in PBS; in mM: 137 NaCl, 2.7 KCl, 8 Na₂HPO₄, 2 KH₂PO₄, pH 7.4) at 4°C to sink overnight. Visual cortex was sectioned into 20 μm coronal slices using a freezing sliding microtome (Leica) and stored in cryoprotectant (20% sucrose, 30% ethylene glycol, 0.02% sodium azide, in sodium phosphate buffer, pH 7.4) at -20°C for <2 months until antibody incubation. The sections were rinsed four times for 5 min each in PBS at room temperature, permeabilized in 2% Triton X-100 in sodium phosphate buffer (50 mM NaH₂PO₄ and 200 mM Na₂HPO₄, pH 7.4), and incubated in -20°C methanol for 10 min. Following four rinses for 5 min each in PBS at room temperature, the sections were incubated in blocking solution (10% normal donkey serum, 1% Triton X-100, 4% bovine serum albumin in PBS) for 1 h at room temperature, and subsequently incubated in primary antibodies diluted in blocking buffer (1:500 rabbit anti-GAD65 polyclonal antibody, Millipore Bioscience Research Reagents; 1:200 mouse anti-NeuN monoclonal antibody, clone A60, Millipore) for 7 d at 4°C. Sections were then rinsed four times for 5 min each in PBS at room temperature and incubated in secondary antibodies diluted 1:200 in 1.5% normal donkey serum in PBS (anti-rabbit Alexa Fluor 488 and anti-mouse Alexa Fluor 633, Invitrogen) for 2 h at room temperature. Sections were rinsed four times for 5 min each before a final wash for 10 min in PBS at room temperature. They were then mounted on precleaned glass slides, air dried overnight in the dark, and coverslipped with mounting solution (ProLong Antifade, Invitrogen).

Fluorescence signals from fluorophore-conjugated secondary antibodies were imaged using a Zeiss LSM510 confocal laser-scanning microscope. Filters and dichroic mirrors were set to detect signals from Alexa Fluor 488 (bandpass filter, 505–530 nm) and Alexa Fluor 633 (long-pass filter, 650 nm) using a dual-scan mode. Sections were imaged using a 63× oil-immersion lens and scanned as z-stacks at 1 μm intervals through the 20 μm thickness. Confocal images were analyzed using Velocity (Improvision) image analysis software. A single section in the middle of the stack (the 10th section from the top) was used for analysis. Sections containing prominent blood vessels were excluded from analysis. The density, size, and intensity of GAD65 puncta as well as the density of NeuN-positive neurons were quantified for each section and averaged across the group. All the imaging and analyses parameters were kept constant across the experimental condition.

RNA extraction and cDNA conversion. Following decapitation, brains were rapidly removed from the skull. Visual and frontal cortices were manually dissected and submerged in RNALater (Life Technologies), and stored at 4°C for 48 h. They were then transferred to Trizol reagent (Life Technologies) and dounce homogenized. Following crude extraction, RNA was further purified on an RNeasy column with on-column DNase treatment performed according to the manufacturer's instructions (Qiagen). One microgram of RNA was converted to cDNA using SuperScript III (Life Technologies) according to the manufacturer's instructions.

Quantitative PCR. Twenty nanograms of reverse transcribed cDNA was used for each reaction with MGB FAM-labeled TaqMan probes (Life Technologies) in 1× Gene Expression Master Mix (Life Technologies). Each reaction was performed in triplicate on a 4S Realplex Mastercycler (Eppendorf). PCR was performed for 40 cycles of 95°C for 15 s and 60°C for 60 s. The primer sequences are as follows: Exon I: forward, CACAT TACCTTCTGCATCTGTTG, reverse, ACCATAGTAAGGAAAAGGA TGGTCAT, probe, 6FAM-AGGCCACAATGTTCCACCAG. Exon II-C: forward, TTGGGAAATGCAAGTGTATCA, reverse, CGAAGTAT GAAATAACCATAGTAAGGAAA, probe, 6FAM-CCGCAAAGAAAGTT CCACCAG. Exon IV: forward, CTGCCTTGATGTTACTTTGACAAG, reverse, ACCATAGTAAGGAAAAGGATGGTCAT, probe, 6FAM-TG ACTGAAAAGTTCCACCAGG; Exon VI: forward, CAGAAGCGTGA

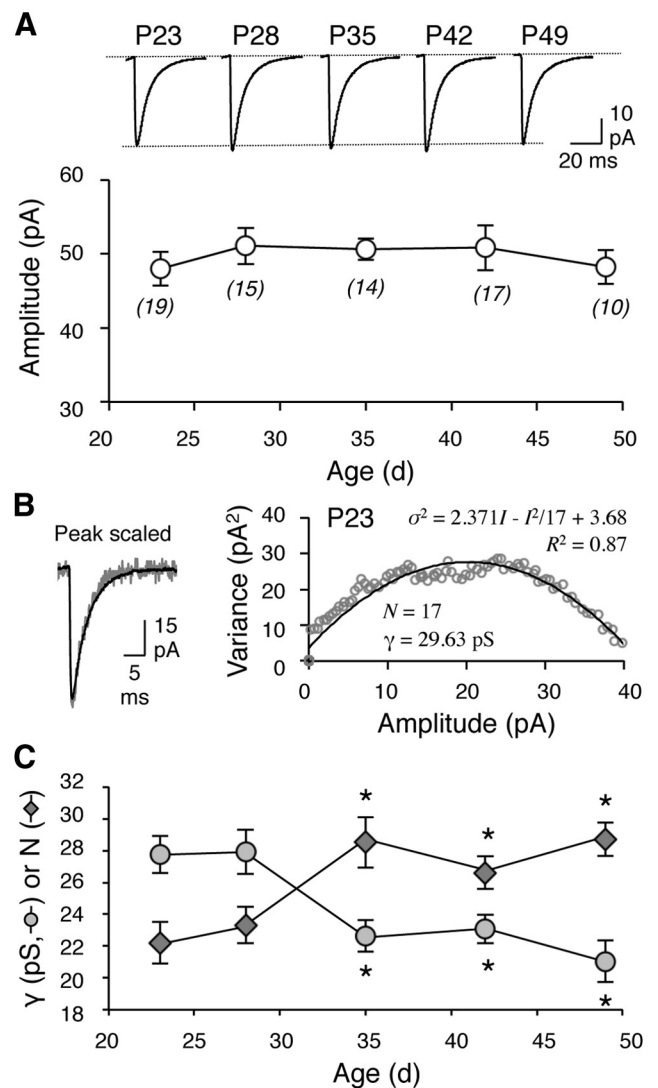


Figure 1. Developmental profile of mIPSC changes in layer 2/3 pyramidal neurons of V1. **A**, The average amplitude of mIPSCs did not change significantly between P21 and P49. The average mIPSC traces are shown in the top panel. The number of cells for each group is indicated in parentheses. For mIPSC parameters, see Table 1. **B**, An example of peak-scaled nonstationary fluctuation analysis of mIPSCs. Left, An average mIPSC trace (black line) superimposed with an individual mIPSC (gray line). Right, Polynomial fit of amplitude variance during the decay phase of the mIPSC for the calculation of single-channel properties. In this example, the data (gray circles) were fitted with a curve (black line) corresponding to the equation shown, which was used to calculate the number of open channels at peak current (N) and the single channel conductance (γ) for this cell. **C**, Developmental change in GABA_AR function. In young mice (P28), layer 2/3 neurons have higher γ (gray circles) and fewer functional GABA_ARs (N ; gray diamonds) than at P35. * $p < 0.05$, ANOVA.

CAACAATGTGA, reverse, ACCATAGTAAGGAAAAGGATGGTCAT, probe, 6FAM-ACCCTGAGTTCACCAGG; Total: forward, TGGCT GACACTTTTGAGCAC, reverse, GGACGCGGACTTGTACACTT. Relative quantification of the template was performed using the $\Delta\Delta C_t$ method, with experimental cDNA normalized to control (*Gapdh*) levels.

Results

Developmental change in postsynaptic GABA_AR function without changes in average mIPSC amplitude

We first determined the developmental profile of mIPSCs in layer 2/3 pyramidal neurons of mouse primary visual cortex. Pharmacologically isolated mIPSCs were recorded in whole-cell voltage-clamp using symmetrical Cl⁻ concentration, which allows the

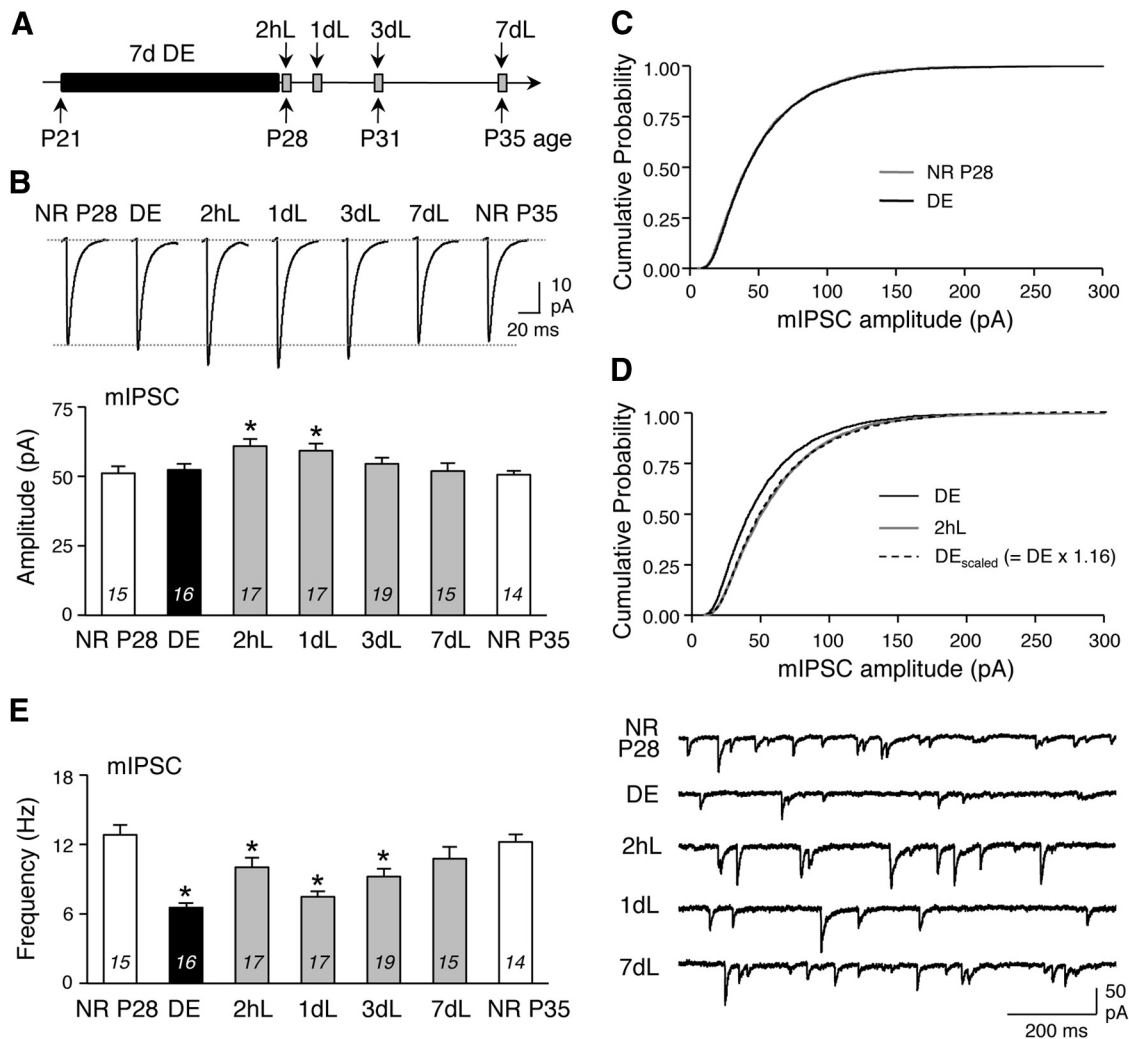


Figure 2. Visual experience triggers rapid rebound potentiation of mIPSCs in juveniles. *A*, Schematics of the experimental paradigm. Seven days of DE was initiated at P21. *B*, Top, Average mIPSC traces from all the cells recorded for each group. Bottom, Comparison of average mIPSC amplitudes across groups. *C*, Cumulative probability of mIPSCs from the NR P28 (gray line) and DE (black line) groups. There was no statistical difference between the two curves ($p = 0.2$, Kolmogorov–Smirnov test), which suggests that there is no change in the distribution of mIPSC amplitude. *D*, The cumulative probability of mIPSC amplitudes of 2hL (gray line) was significantly shifted to larger values compared with those of DE (black line; $p < 0.0001$, Kolmogorov–Smirnov test), which correlates with the increase in average mIPSC amplitude. A scaling factor of 1.16 was derived to match the average mIPSC amplitude of DE to that of 2hL. When the scaling factor was multiplied to an individual mIPSC amplitude of DE (DE_{scaled} ; black dotted line), the cumulative probability was then superimposed with that of 1dL ($p = 0.3$, Kolmogorov–Smirnov test). This demonstrates that the increase in mIPSC amplitude occurred via a global multiplicative scaling mechanism. *E*, Regulation of mIPSC frequency. Left, Comparison of average mIPSC frequency across groups. Right, Example mIPSC traces for each group. The number of cells for each group is indicated inside each bar (*B*, *E*). * $p < 0.05$, ANOVA, significantly different from NR. 2hL, 3dL, and 7dL mice are statistically significantly different from DE mice. For mIPSC parameters, see Table 1.

recording of mIPSCs as inward currents at negative holding potentials (Morales et al., 2002; Gao et al., 2010). We found that the average mIPSC amplitude did not change between the third (~P21) and seventh (~P49) week of postnatal age (Fig. 1A). Nonetheless, postsynaptic GABA_AR function changed during this time period, as revealed by peak-scaled nonstationary fluctuation analysis of the mIPSCs (De Koninck and Mody, 1994; Fig. 1B). Between P28 and P35, the functional properties of the channels open at the peak current changed from a few high-conductance channels to a larger number of lower-conductance channels (Fig. 1C). This suggests a coordinated switch in GABA_AR function such that the average amplitude of mIPSCs remains constant during development. Interestingly, the developmental changes in GABA_AR function terminated at approximately P35, which is also the age at which both the release probability of evoked IPSC and the number of inhibitory syn-

apses reach maturation in these neurons (Huang et al., 1999; Morales et al., 2002; Jiang et al., 2010b).

Rebound potentiation of mIPSC when dark-exposed mice are re-exposed to light

To determine whether mIPSCs are regulated by sensory experience, we exposed mice to darkness for 1 week at P21 (Fig. 2A). One week of DE did not alter the average mIPSC amplitude (Fig. 2B) or the cumulative probability of mIPSC amplitude distribution (Fig. 2C). This is consistent with a previous study showing an absence of change in mIPSC amplitude when mice are dark reared soon after eye opening (Morales et al., 2002). Despite the absence of a change in mIPSC amplitude after DE, re-exposing DE mice for 2hL or 1dL significantly increased the mIPSC amplitude, which gradually returned to normal levels after 3–7 d (Fig. 2B). This is a novel form of inhibitory plasticity where restoring

vision in DE mice produces a rebound potentiation of mIPSCs. The rebound potentiation of average mIPSC amplitude in the 2hL group was due to multiplicative scaling of individual mIPSCs (Fig. 2D), which suggests that this increase occurs globally across the sampled synapses.

The change in visual experience also altered mIPSC frequency, which decreased after DE and recovered gradually after 7dL with a transient partial rebound after 2hL (Fig. 2E). The reversible changes in mIPSC frequency correlated with changes in the density of GAD65 puncta without alterations in puncta size or intensity (Fig. 3). This is consistent with previous findings showing that visual deprivation arrests the developmental increase in inhibitory synapse number, which recovers upon visual experience (Morales et al., 2002; Chattopadhyaya et al., 2004; Kreczko et al., 2009). Together with the lack of an observed change in mIPSC amplitude after DE, this result is consistent with the interpretation that DE prevents the developmental increase in inhibitory synapse number without affecting the strength of individual synapses (Morales et al., 2002). Consistent with this interpretation, we observed a developmental increase in mIPSC frequency between P21 and P28 without any accompanying changes in average mIPSC amplitude (Table 1). The frequency of mIPSCs when DE was initiated at P21 for 1 week was significantly lower than that of NR P21 mice (Table 1). Hence, it is likely that a DE-induced decrease in mIPSC frequency may involve other functional changes in addition to a developmental arrest in inhibitory synapse maturation.

Further analysis of the underlying GABA_AR single-channel properties using peak-scaled nonstationary fluctuation analysis of mIPSCs showed that the rebound potentiation of mIPSC amplitude with light re-exposure is due to an acceleration of the developmental increase in open channel number, which happened quite rapidly even after only 2hL (Fig. 4A). On the other hand, single-channel conductance, which decreases during normal development, was not regulated by changes in visual experience (Fig. 4B). These data demonstrate that the rebound potentiation of mIPSCs after light re-exposure involves the regulation of the functional GABA_AR number. However, this was not accompanied by a change in the cell surface GABA_AR_s as measured using steady-state surface biotinylation of the $\alpha 1$ subunit (Fig. 4C), a major subunit expressed in cortex (Möhler, 2006). In contrast, 2hL significantly increased the total expression levels of GABA_AR $\alpha 1$ and $\beta 2/3$ subunits without significant changes in $\gamma 2$ levels (Fig. 4D). These results suggest that exposure to visual stimuli can rapidly alter the expression of specific GABA_AR subunits.

The rebound potentiation of mIPSC amplitude and changes in GABA_AR function were not observed in mice older than P35 (Fig. 5), which demonstrates that there is a critical period for this form of plasticity. P35 is the age when the normal GABA_AR func-

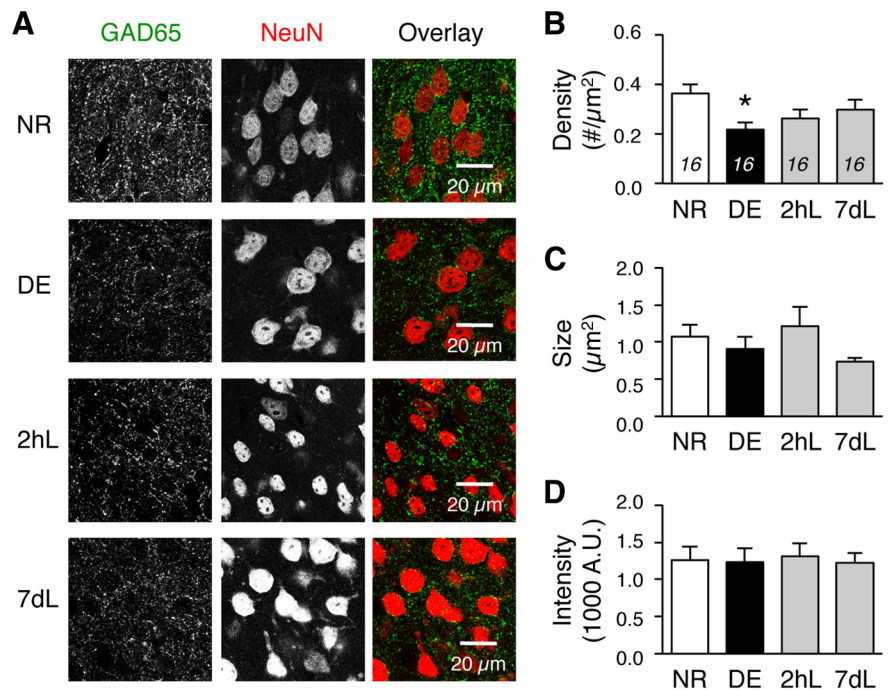


Figure 3. Visual deprivation prevents an increase in GAD65 puncta density in juveniles. **A**, Visual cortex sections were double stained for GAD65 (green) and NeuN (red). Images shown are areas analyzed in layer 2/3 for NR (P28), 7 d DE (initiated at P21), and 2hL or 7dL following DE. **B**, DE group showed significantly less GAD65 puncta density. For each group, $n = 16$ sections from three mice. ANOVA: $p < 0.05$. * $p < 0.01$, compared with NR with Dunnett's *post hoc* test. **C**, **D**, There was no significant difference in the size (**C**) or the intensity (**D**) of GAD65 puncta. Neither was there a difference in the density of NeuN-positive neurons in the analyzed area across the three groups (cell density in $100 \mu\text{m}^2$: NR = 0.24 ± 0.015 ; DE = 0.24 ± 0.015 ; 2hL = 0.24 ± 0.014 ; 7dL = 0.24 ± 0.022).

tional switch is completed (Fig. 4A,B), supporting the idea that visual experience-dependent inhibitory rebound potentiation is likely an acceleration of the developmental process and cannot be triggered once the system is mature.

Visual experience following DE increases BDNF expression

BDNF has been implicated in the development and maturation of inhibition in visual cortex (Huang et al., 1999). Recent studies showed that *Bdnf* transcription from activity-dependent promoter IV plays a critical role in inhibitory synaptic transmission in the prefrontal cortex (Sakata et al., 2009), visual cortex (Hong et al., 2008), and barrel cortex (Jiao et al., 2011). To determine whether activity-dependent BDNF expression plays a role in the visual experience-dependent rebound potentiation of mIPSC amplitude, we first determined whether our experimental manipulation of visual experience alters activity-dependent transcription of *Bdnf*. The *Bdnf* promoters most sensitive to neuronal activity are promoter I and promoter IV. Accordingly, we found that transcripts containing exon I and IV were the most substantially upregulated in the visual cortex of DE mice re-exposed to 2hL (Fig. 6A). There was no significant change in any of the transcript levels in the frontal cortex of the same mice (Fig. 6B), which suggests that the regulation is specific to visual cortex.

Minimal change in basal mIPSCs in BDNF-KIV mice

To determine whether expression of activity-dependent BDNF is necessary for the rebound potentiation of mIPSCs in light re-exposed mice, we used BDNF-KIV mice (Sakata et al., 2009, 2013; Jiao et al., 2011; Martinowich et al., 2011). These mice were engineered to attenuate activity-dependent production of BDNF by insertion of a GFP:STOP cassette in *Bdnf* exon IV (Sakata et al.,

Table 1. Comparison of mIPSC parameters and neuronal properties of wild-type mice

Age	Groups	Amplitude (pA)	Frequency (Hz)	Rise time 10–90% (ms)	τ (ms)	R_{in} (M Ω)	R_{ser} (M Ω)
P21	NR ($n = 19$)	48.0 \pm 2.3	9.4 \pm 0.8*	1.8 \pm 0.03	6.0 \pm 0.3	248 \pm 12	19 \pm 0.9
P28	NR ($n = 15$)	51.1 \pm 2.5	12.8 \pm 0.9	1.7 \pm 0.06	6.0 \pm 0.2	240 \pm 14	19 \pm 0.9
	7dDE ($n = 16$)	52.3 \pm 2.3	6.6 \pm 0.4*	1.6 \pm 0.05	6.0 \pm 0.1	259 \pm 17	18 \pm 1.0
	+2hL ($n = 17$)	60.9 \pm 2.5*	10.0 \pm 0.8*	1.6 \pm 0.06	6.0 \pm 0.2	268 \pm 16	18 \pm 1.0
	+1 dL ($n = 17$)	59.2 \pm 2.5*	7.5 \pm 0.5*	1.7 \pm 0.05	6.2 \pm 0.2	257 \pm 15	19 \pm 0.9
	+3 dL ($n = 19$)	54.5 \pm 2.2	9.2 \pm 0.7*	1.6 \pm 0.05	5.9 \pm 0.2	253 \pm 11	17 \pm 0.6
	+7 dL ($n = 15$)	51.9 \pm 2.9	10.8 \pm 1.0	1.6 \pm 0.05	6.5 \pm 0.3	222 \pm 13	19 \pm 1.1
P35	NR ($n = 14$)	50.6 \pm 1.5	12.2 \pm 0.7	1.8 \pm 0.05	6.2 \pm 0.4	218 \pm 9	21 \pm 0.8

τ , Decay time constant; 7dDE, 7 d of DE; R_{in} , input R ; R_{ser} , series R .

*Statistically different from P28 NR mice with one-way ANOVA ($p < 0.05$) followed by Fisher's PLSD *post hoc* test ($p < 0.05$).

2009). This manipulation completely disrupts the production of BDNF from promoter IV. Further characterization revealed that *Bdnf* transcription from other promoters was also reduced, creating a hypomorph that results in a modest decrease of cortical BDNF, but highly diminished production of BDNF in response to neuronal activity (Martinowich et al., 2011; Sakata et al., 2013). Thus, in these mice there is a nearly complete elimination of the induction of BDNF protein in response to induced neuronal activity (Sakata et al., 2009, 2013; Jiao et al., 2011; Martinowich et al., 2011).

We first examined whether there was any difference in the developmental profile of mIPSCs in layer 2/3 pyramidal neurons of visual cortex between BDNF-KIV and wild-type littermates (BDNF-WT) between P28 and P35. We focused on this age group because the rebound potentiation of mIPSCs is restricted to this age group and is lost after P35 (Fig. 5). Both BDNF-KIV and BDNF-WT mice showed constant mIPSC amplitude at P28 and P35 (Fig. 6C), which is similar to what we observed in our regular wild-type mice (Fig. 1A). While the BDNF-WT mice showed a normal developmental change from the low open channel number with high conductance at P28 to high open channel number with low conductance at P35, BDNF-KIV mice lacked this developmental switch in GABA_AR function (Fig. 6D,E). These results indicate that the apparent normal basal inhibitory synaptic strength in the BDNF-KIV mice masks the underlying deficit in the developmental switch of GABA_AR function. Furthermore, this suggests that the expression of activity-dependent BDNF is required for the developmental switch in GABAergic synaptic transmission.

Visual experience-induced rebound potentiation of mIPSC amplitude is absent in BDNF-KIV mice

Next, we determined the contribution of activity-dependent BDNF expression to visual experience-dependent regulation of mIPSCs. Similar to our previous results, BDNF-WT mice showed significant rebound potentiation of mIPSC amplitude with 2hL and 1dL, which occurred via multiplicative scaling, and also exhibited reversible regulation of mIPSC frequency (Fig. 7A–D). On the other hand, the rebound potentiation of mIPSC amplitude was absent in BDNF-KIV mice, while mIPSC frequency regulation was mostly present, albeit with the loss of transient rebound at 2hL (Fig. 7E–H). This indicates that activity-dependent BDNF production plays a critical role in regulating the rebound potentiation of inhibitory synaptic transmission, but for the most part it is dispensable for mIPSC frequency regulation.

Discussion

Here we report a novel form of inhibitory synaptic plasticity where mIPSCs undergo rebound potentiation via regulation of

GABA_AR function when DE mice are re-exposed to light. This form of inhibitory synaptic plasticity was restricted to a critical period, such that it could not be elicited after P35 when the normal developmental switch in GABA_AR function is complete. Both the developmental switch in GABA_AR function and rebound potentiation of mIPSC amplitude were absent in BDNF-KIV mice, which demonstrates that the expression of activity-dependent BDNF is critical for these processes. However, experience-dependent regulation of mIPSC frequency was largely independent of activity-dependent BDNF expression, which suggests a rather specific role of BDNF in regulating inhibition.

Our results suggest that inhibitory synapses respond asymmetrically to loss of vision versus recovery from visual deprivation. While DE does not alter mIPSC amplitude or GABA_AR function in layer 2/3 of V1, 2hL following DE is able to rapidly increase the GABA_AR open channel number and increase mIPSC amplitude via a multiplicative scaling mechanism. Such asymmetry in response to changes in neural activity is not an isolated case as it is also seen in homeostatic regulation of excitatory synapses. For instance, there is an asymmetry in the time required to homeostatically scale mEPSCs, such that visual deprivation-induced scaling up in layer 2/3 of V1 requires a few days, while re-exposure to light for only a couple of hours is sufficient to scale down mEPSCs (Goel et al., 2006; Goel and Lee, 2007; Gao et al., 2010). Asymmetry in timing is not restricted to synaptic scaling, but is also seen for in the sliding threshold, where the increase in synaptic modification threshold with enhanced neural activity has a faster time course than decreasing the threshold with reduced activity (Quinlan et al., 1999a,b; Philpot et al., 2001). Furthermore, molecular mechanisms of homeostatic regulation of excitatory synapses in V1 show asymmetry as well: scaling up depends on GluA1 phosphorylation of S845 (Goel et al., 2011), while scaling down requires Arc (Gao et al., 2010). Collectively, these findings suggest that increases and decreases in sensory experience are computed and executed via different mechanisms, and that during development an increase in sensory drive requires more urgent adaptation. In addition, it suggests that sensory experience has distinct functional consequences for the normal versus the deprived cortex.

Adaptation to rapid recovery in sensory experience most likely depends on activity-dependent gene products. This is the case in the regulation of mEPSCs, where the immediate early gene *Arc* is critically involved (Gao et al., 2010). Here we find that activity-dependent production of BDNF plays a critical role in rapid scaling up of mIPSCs in a rebound fashion. This form of inhibitory synaptic plasticity was limited to the critical period for ocular dominance plasticity characterized by brief monocular deprivation (MD) (Gordon and Stryker, 1996; Sawtell et al., 2003). Our

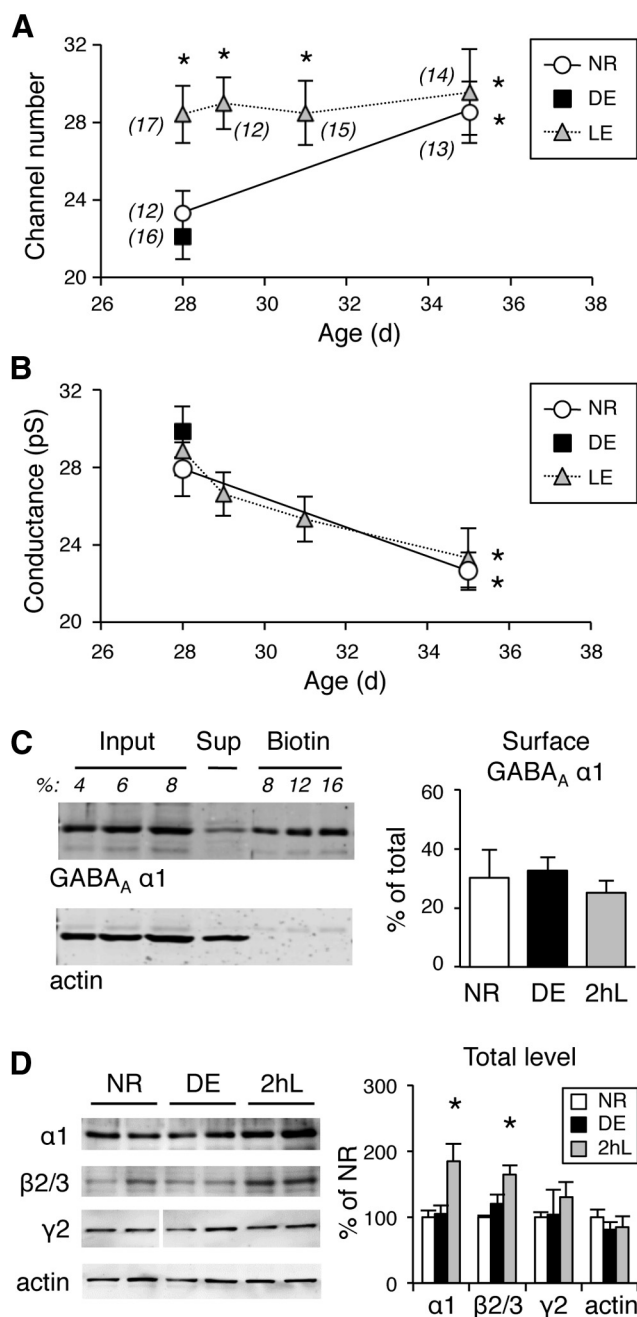


Figure 4. Visual experience-dependent rebound potentiation is correlated with a rapid increase in the number of functional GABA_ARs. **A**, Estimation of the number of GABA_ARs open at peak current (N) using peak-scaled nonstationary fluctuation analysis of mIPSCs. Note the developmental decrease in N between P28 and P35 in NR mice (open circles). Seven days of DE did not alter the N (black square), while 2hL and 1dL significantly increased the N (gray triangles), which reached the N values seen in the P35 NR group (n for each group, shown in parentheses). ANOVA: $p < 0.01$. * $p < 0.05$ from P28 NR with Fisher's PLSD *post hoc* test. **B**, γ Values of GABA_ARs estimated using peak-scaled nonstationary fluctuation analysis of mIPSCs. Note the developmental decrease in γ between P28 and P35 in NR mice (open circles). Seven days of DE did not alter the γ (black square). While subsequent light exposure gradually decreased the γ (gray triangles), which closely followed the developmental decline (n , the same as in **A**). ANOVA: $p < 0.001$. * $p < 0.01$ compared with P28 NR with Fisher's PLSD *post hoc* test. **C**, Measurement of cell surface GABA_ARs using steady-state surface biotinylation. Left, Example immunoblots of total homogenate (Input), intracellular fraction [supernatant (Sup)], and biotinylated cell surface fraction (Biotin). Different amounts of Input and Biotin samples were loaded as shown, and the percentage of cell surface GABA_ARs were calculated from the band intensities. The specificity of surface protein isolation with biotinylation was determined for each blot by simultaneously probing with an antibody against actin (bottom). Note an absence

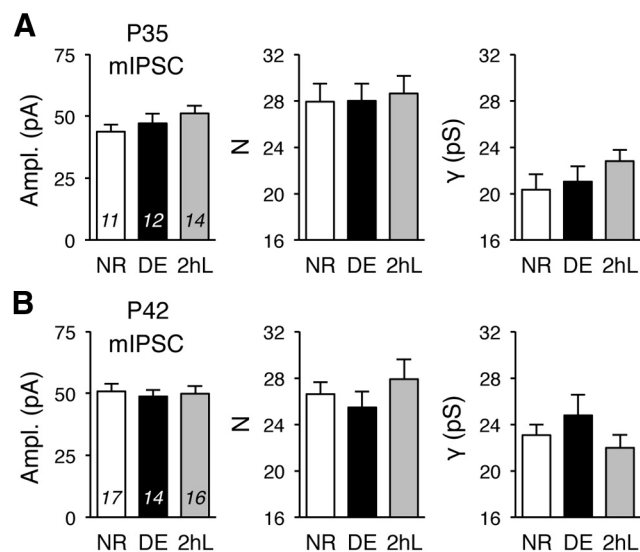


Figure 5. Rebound potentiation of mIPSCs is absent in older animals. **A**, **B**, Comparison of average mIPSC amplitude (left), the number of functional GABA_ARs at N (middle), and γ (right) in NR mice, and adult mice with 7 d of DE and 2hL. Number of cells for each group is indicated inside each bar. **A**, Results from P35 mice. DE was initiated at P28 for 7d. **B**, Results from P42 mice. DE was initiated at P35 for 7d.

description of the inhibitory rebound potentiation is consistent with the notion that BDNF-TrkB signaling plays a more prominent role in recovery from MD, rather than in competition with inputs during MD (Kaneko et al., 2008). It further suggests that activity-dependent *Bdnf* transcription via promoter IV plays a prominent role in strengthening inhibition to limit cortical excitation when vision is recovered. Several previous studies have reported that promoter IV-mediated *Bdnf* expression sculpts inhibition. For example, BDNF-KIV mice show reduced inhibition in both layer 5 of prefrontal cortex (Sakata et al., 2009) and layer 4 of barrel cortex (Jiao et al., 2011) under basal conditions. These results are different from our current study, where we failed to see any significant change in the basal mIPSC amplitude or frequency in the layer 2/3 pyramidal neurons of V1 (Fig. 6C). This discrepancy may stem from the different brain regions or laminae studied, implying potential diversity in promoter IV-mediated BDNF functions. In CREM^{KI} mice, in which CREB binding at promoter IV is disrupted due to a point mutation of the CaRE3/CRE, there was an increase in basal mIPSC amplitude and a reduction in basal mIPSC frequency in layer 2/3 of V1 (Hong et al., 2008). This study was conducted in a younger age group (P16–P18), which is before the opening of the critical period for ocular dominance plasticity (Espinosa and Stryker, 2012; Levelt and Hübener, 2012). Hence, together with our data, this may suggest that there is a developmental effect on the phenotype of basal inhibitory synaptic transmission. This would be consistent with previous studies showing that BDNF expression levels can alter the time course of inhibitory synapse development in V1 (Huang et al., 1999; Gianfranceschi et al., 2003). Our results suggest that even if there is minimal change in basal inhibitory synaptic trans-

←

of actin in the Biotin lanes. Right, Comparison of the average percentage of cell surface GABA_ARs ($n = 5$ mice each group, ANOVA: $p = 0.72$). **D**, Quantification of total expression levels of major GABA_AR subunits. Left, Example immunoblots probed with $\alpha 1$, $\beta 2/3$, $\gamma 2$, and actin. Right, Quantification of the blots. $N = 4–6$ mice per group (ANOVA: $p < 0.01$; * $p < 0.05$ compared with NR controls with Newman–Keuls *post hoc* test).

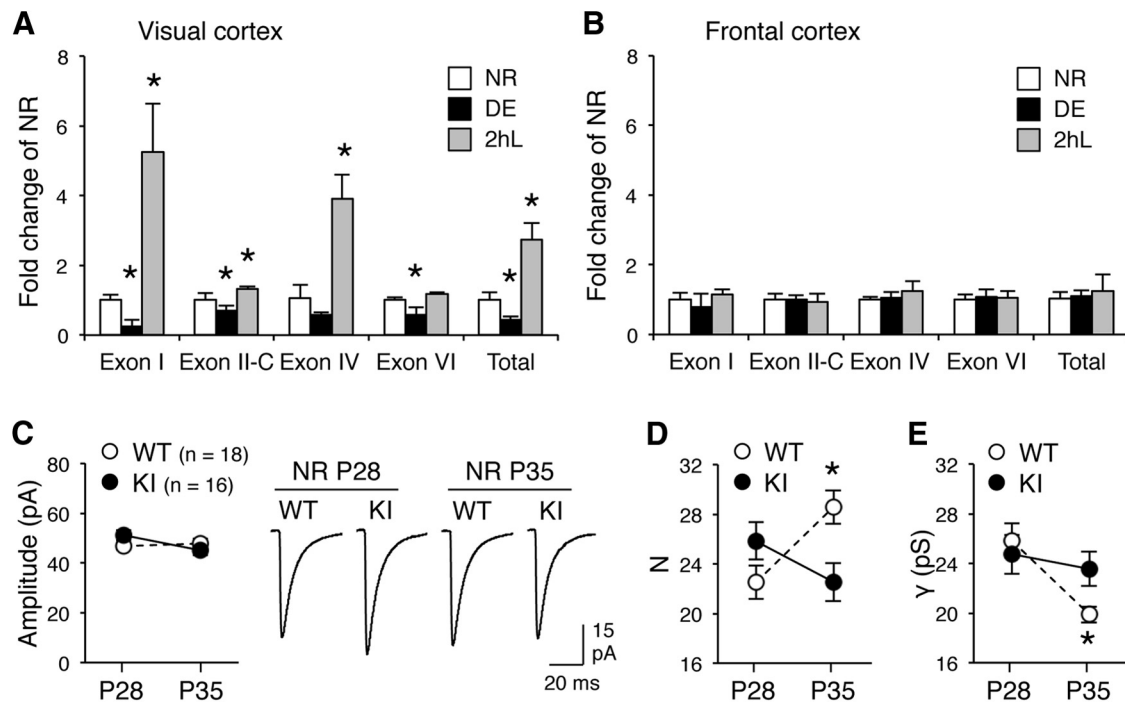


Figure 6. Visual experience increases *Bdnf* transcription, and BDNF-KIV mice lack developmental changes in inhibitory synaptic strength. **A, B**, Comparison of expression of individual exon-containing *Bdnf* transcripts (I, II-C, IV, and VI) and total (*Bdnf* common coding exon) in visual cortex (**A**) and frontal cortex (**B**) of NR mice ($n = 5$ mice), mice with 7 d of DE ($n = 4$ mice), and mice exposed to 2hL ($n = 4$ mice). Note the specific changes in visual cortex without alterations in transcript levels in frontal cortex. $*p < 0.05$, Newman–Keuls *post hoc* test following one-way ANOVA. **C**, Left, Comparison of average mIPSC amplitude between NR WT mice (open circles) and BDNF-KIV mice (KI; black circles) at P28 and P35. The number of cells for each group is shown in parentheses. Right, Average mIPSC traces. **D, E**, Comparison of the mean number of GABA_ARs open at *N* (**D**) and γ (**E**) calculated from nonstationary fluctuation analysis of mIPSCs between WT (open circles) and KI (black circles) mice. Two-way ANOVA: $p < 0.02$ interaction between genotype and age, $*p < 0.05$ between P28 and P35 for each genotype with Newman–Keuls *post hoc* test.

mission in BDNF-KIV mice, there is an underlying defect in the developmental maturation of GABA_AR function. We cannot rule out the possibility that this might have been due to a small general reduction in basal BDNF expression in BDNF-KIV mice.

We have uncovered that there is a coordinated change in GABA_AR channel properties while maintaining constant mIPSC amplitude during the developmental time examined in this study (Fig. 1). Moreover, visual experience-induced rebound potentiation of mIPSC amplitude was restricted to the age before this developmental switch in GABA_AR function is completed (P35). Some *in vitro* studies have suggested that the homeostatic regulation of mIPSC amplitude is due to regulation of vesicular GABA content (Hartman et al., 2006; Hartmann et al., 2008). However, we did not observe significant changes in the rise time of mIPSCs (Table 1), which should decrease with increased GABA release; nor did we see significant changes in GAD65 expression at individual synapses as determined by the lack of a change in GAD65 puncta intensity (Fig. 3). Therefore, rebound potentiation of mIPSC amplitude in our preparation likely reflects postsynaptic changes in GABA_ARs, which are rather complex. We found a rapid increase in the total expression of $\alpha 1$ and $\beta 2/3$ subunits of GABA_ARs with 2hL. Despite the increase in total $\alpha 1$ with 2hL, we did not observe a significant change in its steady-state surface expression. One possibility for this discrepancy is that the kinetics of the surface expression of GABA_AR subunits is increased without alterations in the steady-state level. Another possibility is that steady-state biotinylation may detect only the extrasynaptic pool of GABA_ARs, which is similar to what is estimated for AMPARs (Goel et al., 2011). It is also possible that the change is limited to the synthesis or degradation of GABA_AR subunits. In any case,

our results suggest that GABA_ARs are intricately regulated by vision, which warrants further investigation. While most *in vitro* studies report a reduction in mIPSC amplitude with inactivity (Hartman et al., 2006; Swanwick et al., 2006; Hartmann et al., 2008; Kim and Alger, 2010; Sarti et al., 2013), we did not observe changes in mIPSC amplitude with visual deprivation, but only observed rebound potentiation of mIPSCs when vision was restored. These findings suggest that visual deprivation may not lead to inactivity of the cortical neurons, as would occur with pharmacological inhibition of neurons in reduced preparations, and highlights the potential limitations of *in vitro* systems in modeling *in vivo* conditions.

The age at which the rebound potentiation of mIPSCs is lost coincides with the end of the critical period for ocular dominance plasticity induced by brief MD (Gordon and Stryker, 1996; Sawtell et al., 2003), termination of inhibitory input maturation on layer 2/3 neurons (Morales et al., 2002; Chattopadhyaya et al., 2004; Jiang et al., 2010a), and the developmental decline in synaptic plasticity of thalamocortical afferents to visual cortex (Huang et al., 1999; Jiang et al., 2007). How rebound potentiation of mIPSCs is related to these developmental events will need further examination. Recovery from MD is limited to the same critical period and depends on BDNF-TrkB signaling (Kaneko et al., 2008), suggesting that rebound potentiation may play a role in this process. In any case, the coordinated developmental switch in GABA_AR function requires activity-dependent BDNF production, as it was absent in the BDNF-KIV mice. This suggests that normal visual experience drives activity-dependent transcription of *Bdnf*, which plays a critical role in this aspect of GABAergic maturation. While the detailed mechanisms by which activity-

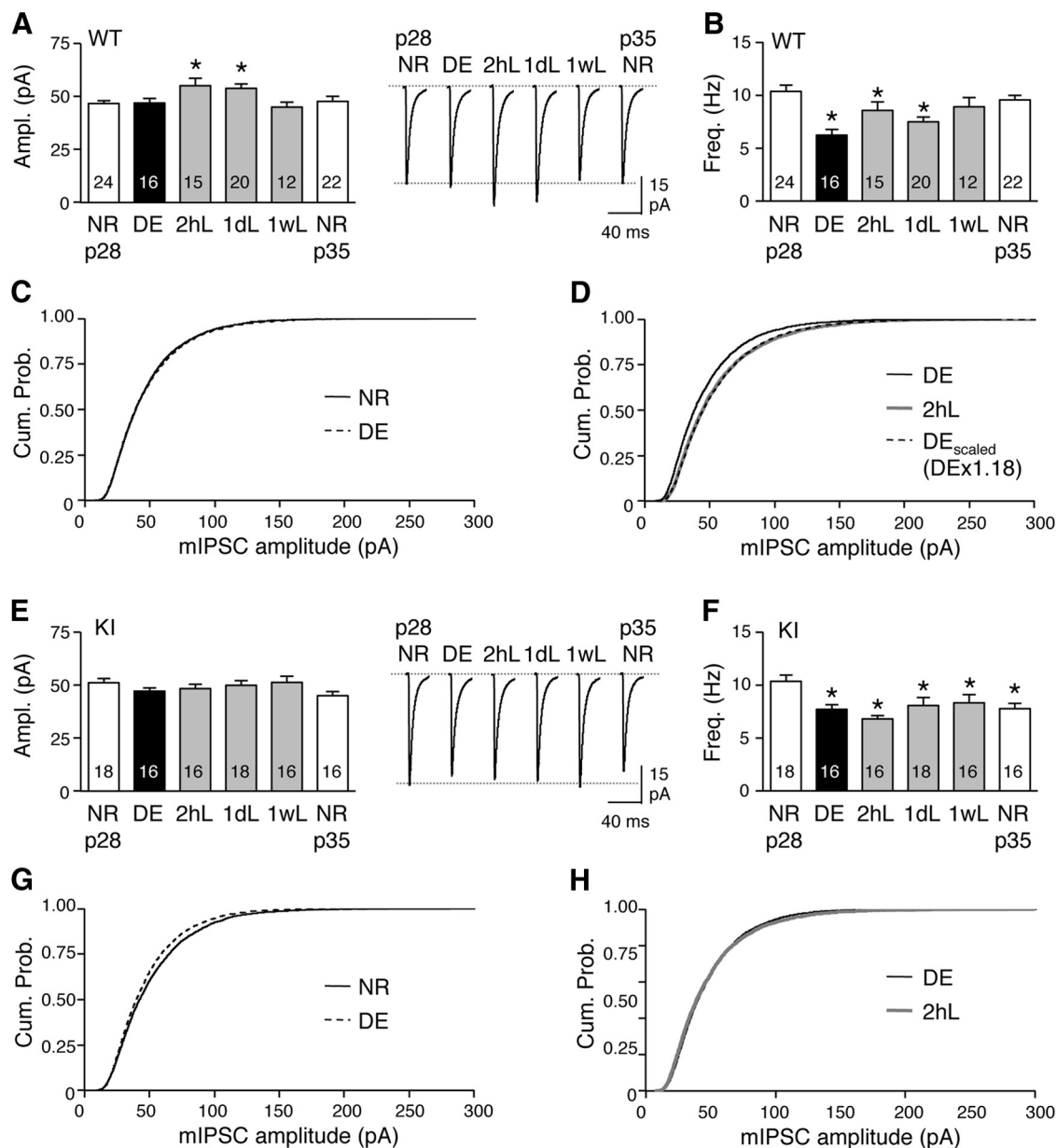


Figure 7. BDNF-KIV mice specifically lack rebound potentiation of mIPSCs with light exposure. **A–D**, Experience-dependent regulation of mIPSC amplitude (**A**, **C**, **D**) and frequency (**B**) in BDNF WT mice. There was no difference in the mIPSC amplitude distribution between NR mice (solid line) and DE mice (dotted line; **C**). The shift in mIPSC distribution to larger values with 2hL (gray line) is multiplicative of DE (black line) values with a scaling factor of 1.18 (DE_{scaled} , dotted line). **E–H**, Lack of rebound potentiation of mIPSC amplitude (**E**, **G**, **H**), while the regulation of mIPSC frequency is largely intact (**F**), in BDNF-KIV (KI) mice. Comparison of cumulative probability (Cum. Prob.) of mIPSC amplitudes (Ampl.) among the NR, DE, and 2hL groups of KI mice (**G**, **H**). The numbers of cells per group are shown inside each bar of **A**, **B**, **E**, and **F**. The average mIPSC traces for each group are shown in the right panels of **A** and **E**. ANOVA: $p < 0.01$; * $p < 0.05$, Multiple-comparisons LSD *post hoc* test. 1wL, Exposed for 1 week to a lighted environment.

dependent BDNF expression regulates GABA_ARs is unknown, there is evidence that the activity-regulated transcription factor Npas4, which upregulates GABA_AR puncta, binds specifically to promoter I and IV to drive *Bdnf* expression (Lin et al., 2008). Hence, the increase in neuronal activity that occurs when vision is restored may upregulate Npas4, which then induces the expression of *Bdnf* via promoters I and IV to increase GABA_AR accumulation at synapses to mediate the rebound potentiation of mIPSCs. It is pertinent to note that the role of activity-dependent BDNF expression is mainly restricted to the postsynaptic regulation of inhibitory function. While both the rebound potentiation of mIPSC amplitude and the developmental switch in GABA_AR function are dependent on vision-induced BDNF, DE-induced

reduction in mIPSC frequency was not (Fig. 7), even if there was a decrease in BDNF expression (Fig. 5A). Therefore, our results underscore a rather specific nature of BDNF action in regulating inhibition, and suggest that presynaptic and postsynaptic function of inhibition can be independently regulated via distinct molecular signaling mechanisms.

References

- Aid T, Kazantseva A, Piirsoo M, Palm K, Timmusk T (2007) Mouse and rat BDNF gene structure and expression revisited. *J Neurosci Res* 85:525–535. CrossRef Medline
- Chattopadhyaya B, Di Cristo G, Higashiyama H, Knott GW, Kuhlman SJ, Welker E, Huang ZJ (2004) Experience and activity-dependent maturation of perisomatic GABAergic innervation in primary visual cortex dur-

- ing a postnatal critical period. *J Neurosci* 24:9598–9611. [CrossRef Medline](#)
- De Koninck Y, Mody I (1994) Noise analysis of miniature IPSCs in adult rat brain slices: properties and modulation of synaptic GABA_A receptor channels. *J Neurophysiol* 71:1318–1335. [Medline](#)
- Espinosa JS, Stryker MP (2012) Development and plasticity of the primary visual cortex. *Neuron* 75:230–249. [CrossRef Medline](#)
- Gao M, Sossa K, Song L, Errington L, Cummings L, Hwang H, Kuhl D, Worley P, Lee HK (2010) A specific requirement of Arc/Arg3.1 for visual experience-induced homeostatic synaptic plasticity in mouse primary visual cortex. *J Neurosci* 30:7168–7178. [CrossRef Medline](#)
- Gianfranceschi L, Siciliano R, Walls J, Morales B, Kirkwood A, Huang ZJ, Tonegawa S, Maffei L (2003) Visual cortex is rescued from the effects of dark rearing by overexpression of BDNF. *Proc Natl Acad Sci U S A* 100:12486–12491. [CrossRef Medline](#)
- Goel A, Lee HK (2007) Persistence of experience-induced homeostatic synaptic plasticity through adulthood in superficial layers of mouse visual cortex. *J Neurosci* 27:6692–6700. [CrossRef Medline](#)
- Goel A, Jiang B, Xu LW, Song L, Kirkwood A, Lee HK (2006) Cross-modal regulation of synaptic AMPA receptors in primary sensory cortices by visual experience. *Nat Neurosci* 9:1001–1003. [CrossRef Medline](#)
- Goel A, Xu LW, Snyder KP, Song L, Goenaga-Vazquez Y, Megill A, Takamiya K, Hugarir RL, Lee HK (2011) Phosphorylation of AMPA receptors is required for sensory deprivation-induced homeostatic synaptic plasticity. *PLoS One* 6:e18264. [CrossRef Medline](#)
- Gordon JA, Stryker MP (1996) Experience-dependent plasticity of binocular responses in the primary visual cortex of the mouse. *J Neurosci* 16:3274–3286. [Medline](#)
- Hartman KN, Pal SK, Burrone J, Murthy VN (2006) Activity-dependent regulation of inhibitory synaptic transmission in hippocampal neurons. *Nat Neurosci* 9:642–649. [CrossRef Medline](#)
- Hartmann K, Bruehl C, Golovko T, Draguhn A (2008) Fast homeostatic plasticity of inhibition via activity-dependent vesicular filling. *PLoS One* 3:e2979. [CrossRef Medline](#)
- Hartveit E, Veruki ML (2007) Studying properties of neurotransmitter receptors by non-stationary noise analysis of spontaneous postsynaptic currents and agonist-evoked responses in outside-out patches. *Nat Protoc* 2:434–448. [CrossRef Medline](#)
- Hong EJ, McCord AE, Greenberg ME (2008) A biological function for the neuronal activity-dependent component of Bdnf transcription in the development of cortical inhibition. *Neuron* 60:610–624. [CrossRef Medline](#)
- Huang ZJ, Kirkwood A, Pizzorusso T, Porciatti V, Morales B, Bear MF, Maffei L, Tonegawa S (1999) BDNF regulates the maturation of inhibition and the critical period of plasticity in mouse visual cortex. *Cell* 98:739–755. [CrossRef Medline](#)
- Jiang B, Huang ZJ, Morales B, Kirkwood A (2005) Maturation of GABAergic transmission and the timing of plasticity in visual cortex. *Brain Res Brain Res Rev* 50:126–133. [CrossRef Medline](#)
- Jiang B, Treviño M, Kirkwood A (2007) Sequential development of long-term potentiation and depression in different layers of the mouse visual cortex. *J Neurosci* 27:9648–9652. [CrossRef Medline](#)
- Jiang B, Sohya K, Sarihi A, Yanagawa Y, Tsumoto T (2010a) Laminar-specific maturation of GABAergic transmission and susceptibility to visual deprivation are related to endocannabinoid sensitivity in mouse visual cortex. *J Neurosci* 30:14261–14272. [CrossRef Medline](#)
- Jiang B, Huang S, de Pasquale R, Millman D, Song L, Lee HK, Tsumoto T, Kirkwood A (2010b) The maturation of GABAergic transmission in visual cortex requires endocannabinoid-mediated LTD of inhibitory inputs during a critical period. *Neuron* 66:248–259. [CrossRef Medline](#)
- Jiao Y, Zhang Z, Zhang C, Wang X, Sakata K, Lu B, Sun QQ (2011) A key mechanism underlying sensory experience-dependent maturation of neocortical GABAergic circuits in vivo. *Proc Natl Acad Sci U S A* 108:12131–12136. [CrossRef Medline](#)
- Kaneko M, Hanover JL, England PM, Stryker MP (2008) TrkB kinase is required for recovery, but not loss, of cortical responses following monocular deprivation. *Nat Neurosci* 11:497–504. [CrossRef Medline](#)
- Kim J, Alger BE (2010) Reduction in endocannabinoid tone is a homeostatic mechanism for specific inhibitory synapses. *Nat Neurosci* 13:592–600. [CrossRef Medline](#)
- Kreczko A, Goel A, Song L, Lee HK (2009) Visual deprivation decreases somatic GAD65 puncta number on layer 2/3 pyramidal neurons in mouse visual cortex. *Neural Plast* 2009:415135. [CrossRef Medline](#)
- Levelt CN, Hübener M (2012) Critical-period plasticity in the visual cortex. *Annu Rev Neurosci* 35:309–330. [CrossRef Medline](#)
- Li YT, Ma WP, Pan CJ, Zhang LI, Tao HW (2012) Broadening of cortical inhibition mediates developmental sharpening of orientation selectivity. *J Neurosci* 32:3981–3991. [CrossRef Medline](#)
- Lin Y, Bloodgood BL, Hauser JL, Lapan AD, Koon AC, Kim TK, Hu LS, Malik AN, Greenberg ME (2008) Activity-dependent regulation of inhibitory synapse development by Npas4. *Nature* 455:1198–1204. [CrossRef Medline](#)
- Maisonpierre PC, Belluscio L, Friedman B, Alderson RF, Wiegand SJ, Furth ME, Lindsay RM, Yancopoulos GD (1990) NT-3, BDNF, and NGF in the developing rat nervous system: parallel as well as reciprocal patterns of expression. *Neuron* 5:501–509. [CrossRef Medline](#)
- Martinowich K, Schloesser RJ, Jimenez DV, Weinberger DR, Lu B (2011) Activity-dependent brain-derived neurotrophic factor expression regulates corticostatin-interneurons and sleep behavior. *Mol Brain* 4:11. [CrossRef Medline](#)
- Möhler H (2006) GABA(A) receptor diversity and pharmacology. *Cell Tissue Res* 326:505–516. [CrossRef Medline](#)
- Morales B, Choi SY, Kirkwood A (2002) Dark rearing alters the development of GABAergic transmission in visual cortex. *J Neurosci* 22:8084–8090. [Medline](#)
- Philpot BD, Sekhar AK, Shouval HZ, Bear MF (2001) Visual experience and deprivation bidirectionally modify the composition and function of NMDA receptors in visual cortex. *Neuron* 29:157–169. [CrossRef Medline](#)
- Quinlan EM, Olstein DH, Bear MF (1999a) Bidirectional, experience-dependent regulation of N-methyl-D-aspartate receptor subunit composition in the rat visual cortex during postnatal development. *Proc Natl Acad Sci U S A* 96:12876–12880. [CrossRef Medline](#)
- Quinlan EM, Philpot BD, Hugarir RL, Bear MF (1999b) Rapid, experience-dependent expression of synaptic NMDA receptors in visual cortex in vivo. *Nat Neurosci* 2:352–357. [CrossRef Medline](#)
- Sakata K, Woo NH, Martinowich K, Greene JS, Schloesser RJ, Shen L, Lu B (2009) Critical role of promoter IV-driven BDNF transcription in GABAergic transmission and synaptic plasticity in the prefrontal cortex. *Proc Natl Acad Sci U S A* 106:5942–5947. [CrossRef Medline](#)
- Sakata K, Martinowich K, Woo NH, Schloesser RJ, Jimenez DV, Ji Y, Shen L, Lu B (2013) Role of activity-dependent BDNF expression in hippocampal-prefrontal cortical regulation of behavioral perseverance. *Proc Natl Acad Sci U S A* 110:15103–15108. [CrossRef Medline](#)
- Sarti F, Zhang Z, Schroeder J, Chen L (2013) Rapid suppression of inhibitory synaptic transmission by retinoic acid. *J Neurosci* 33:11440–11450. [CrossRef Medline](#)
- Sawtell NB, Frenkel MY, Philpot BD, Nakazawa K, Tonegawa S, Bear MF (2003) NMDA receptor-dependent ocular dominance plasticity in adult visual cortex. *Neuron* 38:977–985. [CrossRef Medline](#)
- Swanwick CC, Murthy NR, Kapur J (2006) Activity-dependent scaling of GABAergic synapse strength is regulated by brain-derived neurotrophic factor. *Mol Cell Neurosci* 31:481–492. [CrossRef Medline](#)